Electronic Supplementary Material (ESI) for Energy .

Quantifying the Potential of Ultra-permeable Membranes for Water Desalination

David Cohen-Tanugi, Ronan K McGovern, Shreya H Dave, John H Lienhard and Jeffrey C Grossman

Supplementary Information

Table S1: List of variables and symbols

Symbol	Variable	Units
A_m	Water permeability	$L/(m^2.hr.bar)$
c_b	Bulk feed salinity at position z	mol/L
c_w	Feed salinity at the membrane wall at z	mol/L
R_0	Salt rejection	%
T	Temperature	K
R	Universal gas constant	J/K/mol
ξ	Pressure recovery efficiency	%
η	Pump efficiency	%
E	Specific power consumption per unit of permeate	kWh/m^3
RR	Recovery ratio	%
J	Permeate flux at position z	m/s

k	Mass transfer coefficient	m/s
Q_{in}	Feed flowrate	m^3/d
P_{in}	Feed inlet pressure	bar
π_f	Feed-side osmotic pressure	bar
π_p	Permeate-side osmotic pressure	bar
$\Phi(z)$	Cumulative recovery up to position z	%
L_c	RO vessel length (i.e. number of membrane elements)	m

RO dynamics The flow of feed water parallel to the membrane surface is closely coupled to the flux of permeate water across the membrane. The permeate flux in turn depends on the amount of mixing and the concentration polarization near the membrane. An eddy-promoting feed spacer allows for greater mixing, but it also means that the mass transfer kinetics deviate from traditional results for laminar flow in empty channels[1]. Finally, all these parameters evolve as a function of distance down the RO pressure vessel. The osmotic pressure is higher near the membrane than in the bulk due to concentration polarization[2]. The osmotic pressure difference between the feed and permeate side of the membrane obeys:

$$\Delta\pi(\mathrm{z}) = 2C_b(\mathrm{z})RTR_0 e^{J(\mathrm{z})/k(\mathrm{z})}$$

where k is the mass transfer coefficient that governs the transport of salt away from the membrane surface [2] and all other symbols are defined in Table S1. The derivation of k as a function of local conditions is given below.

Based on the definitions of permeate flux J and osmotic pressure above, it can be shown that J follows:

$$J(\mathrm{z}) = A_m P(\mathrm{z}) - k(\mathrm{z})\mathcal{W}\left(\frac{2C_b(\mathrm{z})\mathrm{e}^{\frac{A_m P(\mathrm{z})}{k(\mathrm{z})}} A_m R R_0 T}{k(\mathrm{z})}\right)$$

where $\mathcal{W}(\mathrm{x})$ is the principal solution for w in the equation $w = w\, e^w$ and is called the Lambert W function, or the *product logarithm* function. Its values are readily computed using *Mathematica 9*.

The net driving pressure and the permeate flux both decline along the vessel length due to increasing feed salinity and viscous losses. Illustrative values for the local feed flowrate, pressure, recovery and salt concentration as a function of z are shown in Figure S1. The figures compare 1.5 versus 15 L/m^2-hr-bar for SWRO. The thin lines in the $P(z)$ plot represent the feed osmotic pressure as a function of distance. At some distance down the RO vessel, the osmotic pressure reaches the hydraulic pressure and the recovery curve becomes flat.

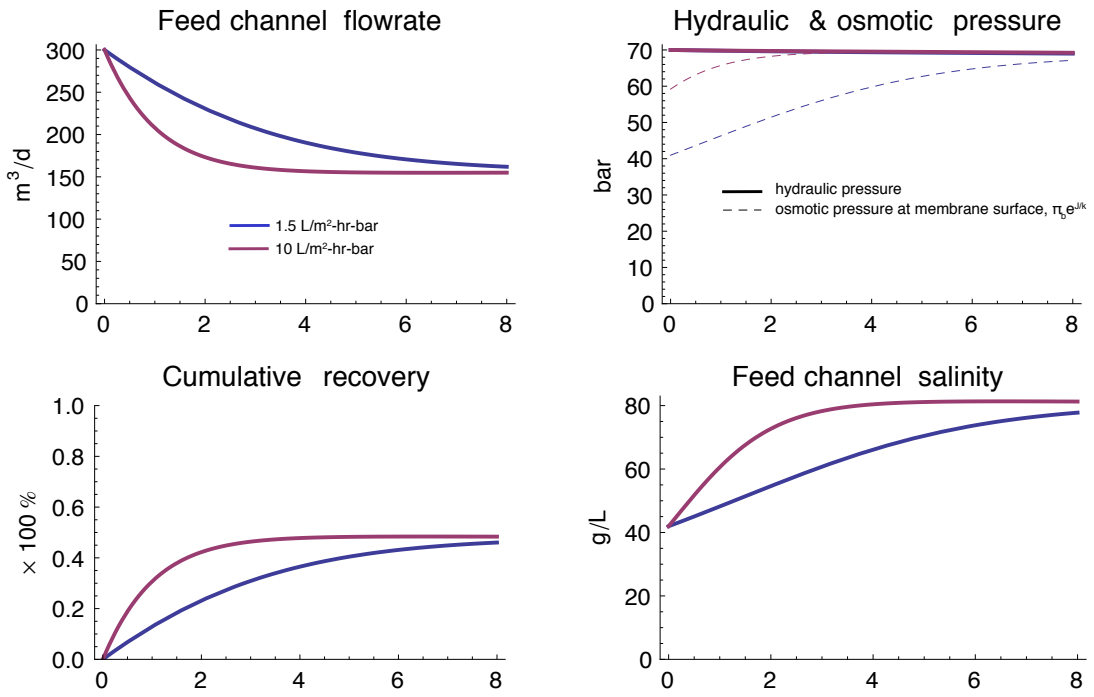

Figure S1: Permeate flowrate, hydrostatic pressure, cumulative permeate recovery and bulk feed salinity as a function of position for seawater at 1.5 vs. 15 L/m^2-hr-bar.

Energy consumption The specific energy consumption of an RO desalination process (expressed in kWh per m^3 of permeate) depends on the flowrate of permeate water (in m^3/day) and on the energy consumption of the pump (in kWh/day), which itself is a function of the required inlet pressure and the pump efficiency η (taken here to be 75%). In the absence of a pressure recovery scheme, no energy is recovered from the pressurized brine and the energy consumption per unit of permeate is simply[3]:

$$E = \frac{W}{Q_{out}} = \frac{1}{\mathrm{RR}} \frac{P_{in}}{\eta}$$

When a pressure recovery device is available to recycle the energy from the brine, the energy consumption becomes[3]:

$$E = \frac{1}{\eta}\frac{P_{in} - \xi(1 - \mathrm{RR})(P_{in} - \mathrm{P}_{lost})}{\mathrm{RR}}$$

Here ξ is the efficiency of the pressure recovery process and is taken to equal 97%. The first term corresponds to the energy required to pressurize the feed water to the inlet pressure, and the second term corresponds to the energy 'recovered' from the brine whose pressure equals $(P_{in} - \mathrm{P}_{lost})$ after accounting for viscous losses. We assume that the high-pressure pump and the circulation pump have the same efficiency η and that the PRD efficiency is ξ = 98%. Salt and water leakage effects across the PRD interface are neglected.

Mass transfer coefficient The mass transfer coefficient k governs the extent of concentration polarization. It depends on the solute diffusivity $\mathcal{D}$ as well on the Reynolds number and the presence of feed spacers that promote mixing by creating eddies in the feed channel. In order to estimate the mass transfer coefficient at a given set of flow conditions, we adapt data from Li et al. for the Sherwood, Power and Reynolds numbers in RO channels in the presence of feed spacer[4]. By fitting the data from Li et al. using power laws, we obtain the following empirical relations for mass transfer:

$$\mathrm{Sh} = 2.53\mathrm{Pn}^{0.2362}$$

$$\mathrm{Pn} = 1.5\mathrm{Re}^{2.78} + 14.2\mathrm{Re}^{2}$$

Here, the Sherwood, Reynolds and Power numbers are defined according to $\mathrm{Sh} = \frac{kH_c}{\mathcal{D}}$, $\mathrm{Re} = \frac{uH_c\rho}{\mu}$, and $\mathrm{Pn} = f\mathrm{Re}^3$ respectively, where f is the Fanning friction factor. The coefficients used here correspond to the traditional case in which the mesh filaments are spaced $H_c/4$ apart from each other and a flow attack angle of 30˚. Rewriting the latter relation in terms of the friction factor gives an expression for f as a function of the feed velocity u:

$$f = \frac{\mu^3\left(\frac{16.H_c^2u^2\rho^2}{\mu^2} + 0.4892\left(\frac{H_cu\rho}{\mu}\right)^{2.964}\right)}{H_c^3u^3\rho^3}$$

From the relation between Sherwood number and Power number, we finally obtain the expression for the mass transfer coefficient in the presence of feed spacers as a function of fluid properties (salt diffusivity, density and viscosity), local feed flowrate and channel height:

$$k = \frac{2.53\mathcal{D}\left(\frac{fH_c^3u^3\rho^3}{\mu^3}\right)^{0.2362}}{H_c}$$

$$= \frac{2.53\mathcal{D}\left(\frac{16.H_c^2u^2\rho^2}{\mu^2} + 0.4892\left(\frac{H_cu\rho}{\mu}\right)^{2.964}\right)^{0.2362}}{H_c}$$

Concentration polarization factor The CPF typically starts at a maximum value at the membrane inlet and decays asymptotically to unity for further distances.

Table S2: Maximum concentration polarization factor for each scenario

CPF	Baseline	Maximizing throughput	Higher throughput	Minimizing pressure	Maximizing recovery
Fixed quantities	N/A	P, RR	E, RR	Q_{in}, RR	Q_{in}, P
Brackish	1.08	1.26	N/A	1.24	1.91
Seawater	1.10	1.44	1.61	1.50	1.65
Flowback water	1.06	1.16	1.19	1.15	1.20

Viscous pressure loss. In a normal RO system, the pressure losses are small (< 5 bar), but they can become non-negligible at higher feed flow rates. The viscous pressure loss per unit distance along the feed channel depends on the feed flowrate. Its exact value differs from the (simpler) traditional expression pure laminar flow due to the presence of eddy promoters. Given that the Fanning friction factor is defined as $f = \frac{\mathrm{Pn}}{\mathrm{Reynolds}^3}$ and that the pressure drop across a pipe of length L equals $\Delta \mathrm{P} = 2\rho f u^2 (\frac{L}{H_c})$, we use the expression for Pn derived above to find:

$$\frac{dP_{lost}(Q)}{dx} = \frac{2W_c\mu^3\left(\frac{16Q^2\rho^2}{W_c^2\mu^2} + 0.489\left(\frac{Q\rho}{W_c\mu}\right)^{2.964}\right)}{H_c^3 Q\rho^2}$$

The total pressure loss as a function of feed flowrate is plotted below for each case analyzed in this paper.

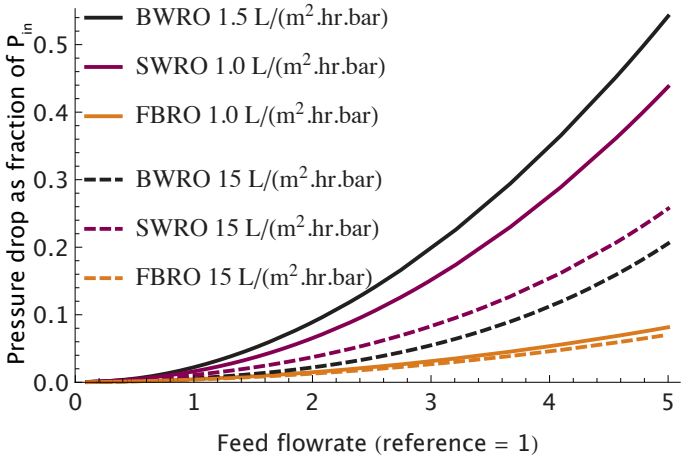

Figure S2: Pressure drop from RO vessel inlet to outlet as a function of feed flowrate.

The figure below indicates that flowrates that would be prohibitive in conventional TFC membranes (e.g. >2x the reference flowrate for BWRO) result in much less significant pressure losses in UPMs. This is due to the steeper permeate flux profile in UPMs, which results in less viscous losses past the RO vessel entrance. But pressure losses are most significant for SWRO: 30% of the pressure becomes dissipated in the vessel at 5x the reference flowrate. This observation is consistent with the energy penalty reported above when operating at high feed flowrates and constant pressures.

Capital costs of SWRO

The typical capital costs for a 150,000 m^3/d SWRO plant with conventional TFC membranes, as predicted by the industry data provider Global Water Intelligence (DesalData.com), are shown in Table S3. The cost factors that scale directly with number of membrane elements (assuming that UPMs cost the same on a per area basis as TFC membranes) are membranes and piping/high alloy, which account for 20% of the capital cost.

Table S3: Predicted capital costs for a 150,000 m^3/d SWRO desalination plant with conventional TFC membranes (Source: Global Water Initiative, desaldata.com)

Factors	Adjusted capital cost	Percent
Intake / outfall	$11,877,940	7.1%
Pumps	$15,271,640	9.1%
Pretreatment	$13,702,060	8.2%
Installation and services	$13,574,790	8.1%
PVs	$2,545,280	1.5%
Design and professional costs	$9,672,040	5.8%
Membranes	$9,332,670	5.6%
Piping/high alloy	$23,755,880	14.2%
Civil engineering	$28,846,430	17.2%
Equipment and materials	$37,415,520	22.3%
Legal and professional	$1,612,010	1.0%
Total	**$167,606,260**	**100.0%**

The total capital cost (~$168,000,000) provided in Table S3 amounts to a normalized capital cost of ($168,000,000)/(150,000 m^3/d) = $1,117 per ($m^3$/d). Assuming typical a 5% discount rate and a 30 year plant life, the levelized capital cost then equals{Rosenboom:2011wi}:

$$1{,}117\ \$/(\mathrm{m}^3/\mathrm{d}) \times (365\ \mathrm{d/yr})^{-1} \times \left(\frac{1-0.95^{30}}{1-0.95}\right) \approx 0.20\ \$/\mathrm{m}^3.$$

Flowback RO

In addition to the two feed water cases examined in the paper, we also considered the effect of UPMs on representative flowback or produced water from hydrocarbon production (80,000 ppm). The reference case corresponded to a feed pressure of 85 bar, 4 membrane elements per vessel, a feed flowrate of 190 m^3/d per vessel, 15% recovery and a membrane permeability of 1.0 L/m^2.hr.bar [5].

Our analysis indicates that more permeable membranes would not greatly lower the energy consumption of FBRO. Keeping recovery ratio, feed flowrate and vessel geometry fixed, a tripling of membrane permeability would only result in a 4% decrease in feed pressure and a 10% decrease in energy consumption. We attribute this finding to the fact that the osmotic limit for FBRO is extremely high (80 bar) due to the salinity of the feed, so that further improvements in membrane permeability would thus have a negligible effect on energy consumption. However, we also find that a tripling in

membrane permeability at the reference feed pressure would enhance permeate recovery by 23% percent.

With regard to equipment requirements, the figure below shows that for FBRO water (with RR = 15%, P_{in} = 85 bar and 4 elements per vessel), tripling the membrane permeability would allow for 56% fewer pressure vessels for a given plant capacity by increasing the permeate production per vessel by 129%. The energy penalty associated with the higher throughput is 6%. Meanwhile, a similar comparison at fixed energy consumption and higher recovery yields a 39% reduction in the required number of pressure vessels. Finally, we find that UPMs could alternatively carry out the RO process for flowback water using only two membrane elements per vessel, compared with four elements in the reference case. For FBRO applications, the lack of financial information about the cost of RO for such applications today makes it unclear whether UPMs would make RO an economically viable solution for flowback water treatment. More research into the engineering and economics of FBRO will be required to fully answer this question, although this work has shown that UPMs could reduce the number of required pressure vessels by 39%, decrease the energy consumption of the RO stage by 10% or increase the permeate recovery from 15% to 19%.

Effect of UPMS on Elements per Vessel in SWRO

UPMs could also allow for higher permeate recovery or a reduction in the number of membrane elements per pressure vessel. In particular, we find that UPMs can reduce the

number of membrane elements in each pressure vessel. In this case, the geometry of individual membrane elements would remain unchanged, and a pressure vessel would be designed to enclose fewer elements in series, each of which would operate at higher flux. The number of membrane elements per pressure vessel at fixed values of feed pressure, flowrate and recovery is plotted in Figure S3. The figure indicates that SWRO vessels could carry out the RO process using only four membrane elements, which is 50% fewer than standard pressure vessels today.

Effect of UPMs on Recovery and Vessel Length in BWRO

The use of UPMs could increase permeate recovery in BWRO by 32% (to 85%, compared with 65% in the reference case) and simultaneously lower energy consumption by 24%. In this case, the feed flowrate, inlet pressure and pressure vessel dimensions would remain unchanged, and the added permeability would allow for greater permeate flux. The energy consumption would decrease because our reference BWRO system does not include a pressure recovery stage, meaning that lower in brine production entails less energy discharge to the environment. Finally, the figure below shows that if the permeate production per vessel were instead left unchanged, each vessel could carry out the RO process using only 3 UPM elements, compared with 7 elements today.

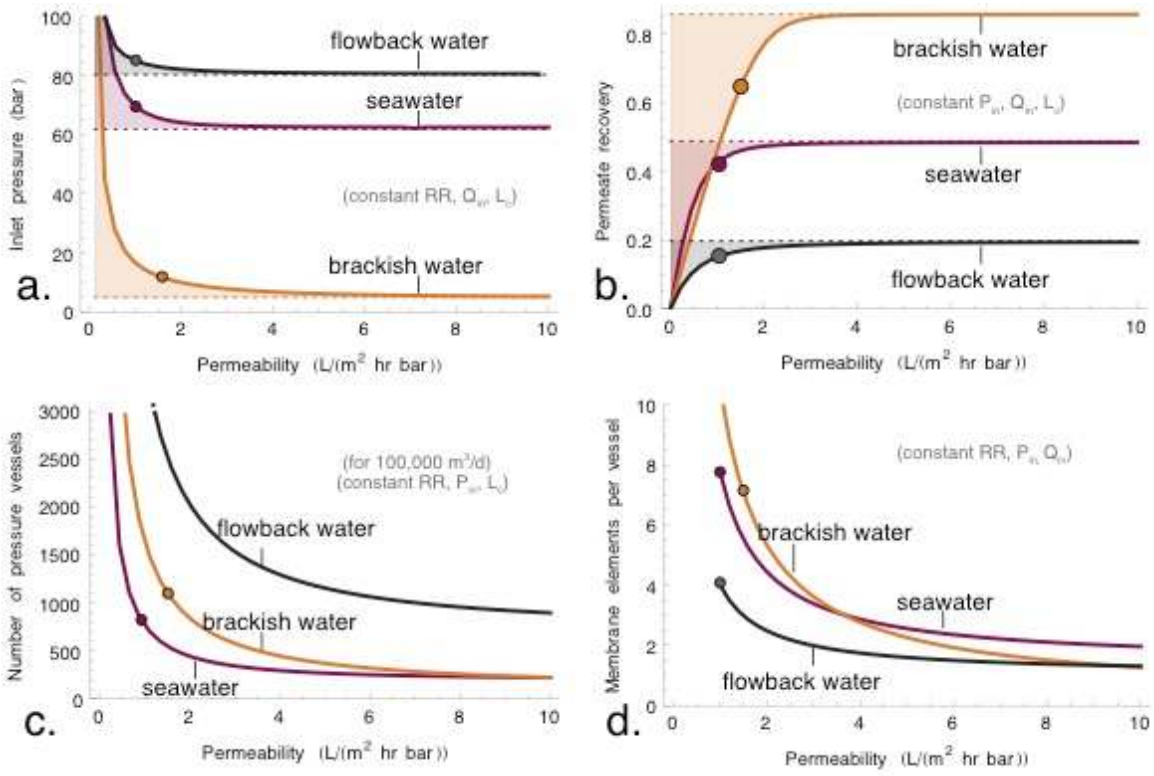

Figure S3: Improvements in key performance criteria as a function of membrane permeability for SWRO at 42,000 ppm NaCl (purple), BWRO at 2,000 ppm NaCl (orange) and FBRO at 80,000 ppm NaCl (black). a) Minimum required inlet pressure and energy consumption as a function of membrane permeability at fixed recovery and feed flowrate. The pressure curves decrease asymptotically to a minimum dictated by the osmotic pressure of the feed water (dotted lines). b) Permeate recovery at fixed feed flowrate and pressure as a function of membrane permeability. Solid lines represent the actual recovery ratio, and dotted lines represent the maximum recovery achievable given the feed salinity and inlet pressure. c) Number of pressure vessels required as a function of membrane permeability for a total capacity of 100,000 m_3/d at fixed recovery ratio and

pressure. d) Number of RO elements per pressure vessel length at fixed recovery ratio, pressure and feed flowrate as a function of membrane permeability. UPMs would allow for RO vessels with fewer membrane elements because the flux across each section of membrane would be higher.

However, we did not consider the benefits from higher recovery or fewer membranes per pressure vessel in the main body of this paper because the value of these improvements is uncertain. While a higher recovery ratio would reduce the total volume of feed water to be pretreated, the higher concentration of the resulting brine makes the overall benefits difficult to estimate. Likewise, shorter RO vessels with fewer elements could allow for compact desalination systems as well as reduced viscous losses along the length of the module, but such vessels would also require an extensive re-engineering of RO systems; the overall benefit from such a change is uncertain as well.

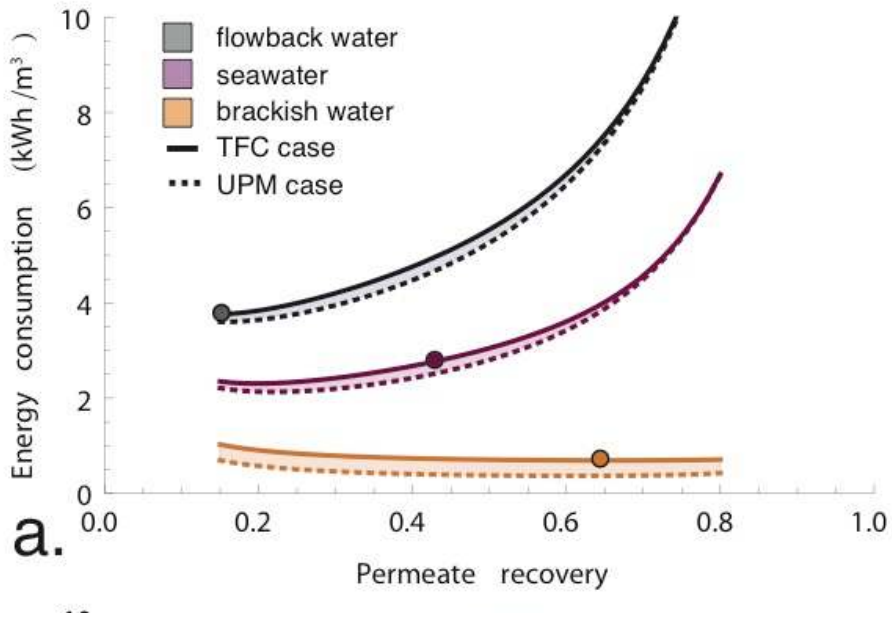

Figure S4: Tradeoff between lower energy and higher recovery ratio at feed flowrate. Energy consumption and recovery ratio are represented on independent axes for a fixed feed flowrate and membrane area. For each scenario, the operating regimes achievable using UPMs (dashed lines) can be compared with those achievable with TFC membranes (solid lines). For example, a BWRO plant could either increase its overall permeate production by 14% (keeping energy consumption unchanged) or reduce its specific energy consumption by 46% without modifying its throughput.

References

1. A. R. Da Costa, A. G. Fane, C. J. D. Fell, and A. C. M. Franken, *J Membrane Sci*, 1991, **62**, 275–291.
2. E. Hoek, A. S. Kim, and M. Elimelech, *Environ Eng Sci*, 2002, **19**, 357–372.

3. C. Liu, K. Rainwater, and L. Song, *Desalination*, 2011, **276**, 352–358.
4. F. Li, W. Meindersma, A. B. De Haan, and T. Reith, *Science*, 2002, **208**, 289–302.
5. D. Yoxtheimer, Brussels, 2011.